Received: 7 September 2023 | Revised: 9 January 2024 | Accepted: 19 January 2024

DOI: 10.1002/biot.202300469

Biotechnology Journal

RESEARCH ARTICLE

Encapsulation of pristine and silica-coated human adipose-derived mesenchymal stem cells in gelatin colloidal hydrogels for tissue engineering and bioprinting applications

Marta M. Maciel[1,2] | Negar Hassani Besheli[2] | Tiago R. Correia[3] | João F. Mano[3] | Sander C. G. Leeuwenburgh[2]

[1]CEB, Campus de Gualtar, Centre of Biological Engineering University of Minho, Braga, Portugal

[2]Department of Dentistry – Regenerative Biomaterials, Radboudumc, Nijmegen, The Netherlands

[3]CICECO, Aveiro Institute of Materials, Department of Chemistry, University of Aveiro, Complexo de Laboratórios Tecnológicos Campus Universitário de Santiago, Aveiro, Portugal

Correspondence
Sander C. G. Leeuwenburgh, Department of Dentistry – Regenerative Biomaterials, Radboudumc, Philips van Leydenlaan 25, 6525 EX Nijmegen, The Netherlands.
Email: sander.leeuwenburgh@radboudumc.nl

Abstract

Colloidal gels assembled from gelatin nanoparticles (GNPs) as particulate building blocks show strong promise to solve challenges in cell delivery and biofabrication, such as low cell survival and limited spatial retention. These gels offer evident advantages to facilitate cell encapsulation, but research on this topic is still limited, which hampers our understanding of the relationship between the physicochemical and biological properties of cell-laden colloidal gels. Human adipose-derived mesenchymal stem cells were successfully encapsulated in gelatin colloidal gels and evaluated their mechanical and biological performance over 7 days. The cells dispersed well within the gels without compromising gel cohesiveness, remained viable, and spread throughout the gels. Cells partially coated with silica were introduced into these gels, which increased their storage moduli and decreased their self-healing capacity after 7 days. This finding demonstrates the ability to modulate gel stiffness by incorporating cells partially coated with silica, without altering the solid content or introducing additional particles. Our work presents an efficient method for cell encapsulation while preserving gel integrity, expanding the applicability of colloidal hydrogels for tissue engineering and bioprinting. Overall, our study contributes to the design of improved cell delivery systems and biofabrication techniques.

KEYWORDS
cell encapsulation, cell-laden hydrogels, colloidal gels, particulate systems, rheology, self-healing

1 | INTRODUCTION

Persisting challenges in achieving functional biomaterial-based constructs with sufficient host compatibility have resulted in low success rates in translating cell-free products to clinical applications.[1] In the last decade, tissue engineering and bioprinting strategies have accelerated the progress regarding more integrative approaches to achieving tissue regeneration by combining cells and biomaterials as opposed to cell-free engineered structures. This recent trend is based on the early integration of cells with biomaterials acting as a supportive system for cell delivery and guidance during subsequent regenerative processes without compromising the natural cellular

Marta M. Maciel and Negar Hassani Besheli contributed equally to this work as shared first authors.

Joao F. Mano and Sander C. G. Leeuwenburgh contributed equally to this work as shared last authors.

organization and function.[2] As such, biomaterials should recapitulate the main functionalities of the native extracellular matrix (ECM) and act as a template facilitating spatial confinement of embedded cells and orchestration of crucial cellular processes such as migration, proliferation, and differentiation.

While various types of biomaterials aim to replicate specific features of the ECM, hydrogels have gained particular attention due to their excellent versatility.[3] Hydrogels are 3D polymeric crosslinked networks that can absorb and retain significant amounts of water, which enables the integration of cells, biomolecules, and/or biofunctional micro/nanoparticles.[4,5] Their main potential resides in the ability to fine-tune both the chemical and physical properties of hydrogels, which broadens their applicability and enhances their similarity to the ECM.

Recently, hydrogels are increasingly considered as bioink formulations for bioprinting and minimally invasive injectable cell delivery systems.[6,7] Traditional bulk hydrogels are characterized by limited nutrient/oxygen diffusion and microporosity, which can be circumvented by the incorporation of nutrient and oxygen carriers or through further structural optimization.[3] However, the most critical factor in the formulation and design of these systems entails cell encapsulation. Besides ensuring cell survival, proliferation, and migration, hydrogels should also offer protection to cells against environmental factors. For example, during minimally invasive delivery/bioprinting strategies, extrusion processes through narrow needles can compromise cell survival due to the high shear stresses exerted by hydrogels on cells.[8] Moreover, other factors like temperature, pH, or crosslinking methods may also negatively affect cell viability.[9] Therefore, hydrogel gelation protocols should be considerably modified to enable cell encapsulation, which stresses the need for novel hydrogel formulations with simplified cell encapsulation opportunities by improving their injectability and printing resolution.[3,10] To address this challenge, two main strategies can be adopted: (i) encapsulation of cells within colloidal instead of monolithic gels and/or (ii) modifying cells to enhance their survival, delivering biochemical cues and/or provide additional protection against high stresses associated with extrusion through narrow needles.[9]

Colloidal (hydro)gels represent a recently emerging and promising alternative to traditional bulk/monolithic hydrogels due to their unique self-healing, shear thinning, and viscoelastic properties.[11] These gels are formed through reversible and noncovalent interparticle interactions such as electrostatic or hydrophobic interactions, forming an arrested network of percolated (nano)particles.[12,13] The reversible bonds between nanoparticles as building blocks ensure that colloidal gel networks exhibit an adaptable and dynamic nature, which not only offers an attractive microenvironment for cell and tissue ingrowth [12,14,15] but also contributes to their shear-thinning, self-healing, and viscoelastic properties. As a result, the high shear stresses exerted on cells during bioink extrusion through narrow needles can be reduced whereafter the gel quickly recovers, to restore its cohesiveness.

Gelatin colloidal gels have received specific attention owing to their favorable physiochemical and biological features that can benefit cell and tissue function for a wide range of potential applications in regenerative medicine. Gelatin, a natural polymer derived from the denaturation of collagen, is highly biocompatible, less antigenic than collagen, readily available, and cost-effective. It has a high degree of biodegradability by enzymes naturally present in the human body and contains adhesion sequences, such as arginine-glycine-aspartic (RGD) sequences, which facilitate rapid cell adhesion to gelatin-based materials. Furthermore, gelatin can be blended with other materials and chemically modified expanding its versatile application in the biomedical field.[16]

Despite the potential benefits of gelatin colloidal gels for cell delivery systems, only a few studies[17,18] have explored the feasibility of incorporating cells into these gels. In fact, most of these studies on gelatin colloidal gels have primarily focused on in vitro tests where cells are seeded on top of the gels.[17,19–22] However, the results from these 2D cell cultures do not accurately reflect the behavior of cells encapsulated within such colloidal gels. Consequently, they fail to provide a direct correlation of cell behavior particularly in the context of tissue engineering, bioprinting applications, and other 3D tissue engineering approaches such as disease models where cells are an integral part of the system.[23] Consequently, interactions between cells encapsulated in gelatin colloidal gels remain poorly understood, although cell encapsulation can strongly affect processes such as gelation kinetics and resulting viscoelastic properties.[10] Hydrogels can offer functional advantages, for instance by protecting cells from harsh environmental conditions such as high shear stresses. However, cells, as another component of the 3D systems, can also be modified to (i) further sustain and improve their survival and viability, (ii) act as a drug delivery system, or (iii) provide biochemical cues.

Here, we evaluated how the encapsulation of cells in gelatin colloidal gels impacted cell viability and the mechanical properties of these cell-laden systems.[24] Human adipose-derived mesenchymal stem cells were deliberately selected since they are easily obtainable and possess regenerative properties similar to other types of mesenchymal stem cells.[25] Moreover, we encapsulated human adipose-derived mesenchymal stem cells partially coated with silica in gelatin colloidal gels to further understand their modulatory potential. The goal was to explore a novel strategy to modulate the mechanical properties of the gel without the need for further post-processing steps or increasing the complexity of the system with other building blocks. These cells partially coated with silica were previously shown to exhibit higher viability when cultured in suspension and a higher degree of protection during extrusion, thereby enhancing cell survival.[24] Additionally, silica can be modified to serve as a drug delivery system and provide specific biochemical cues.

2 | RESULTS AND DISCUSSION

2.1 | Gelatin nanoparticles

Gelatin nanoparticles (GNPs) were produced using a desolvation process and subsequently stabilized through glutaraldehyde crosslinking. The synthesized GNPs were characterized in terms of their size

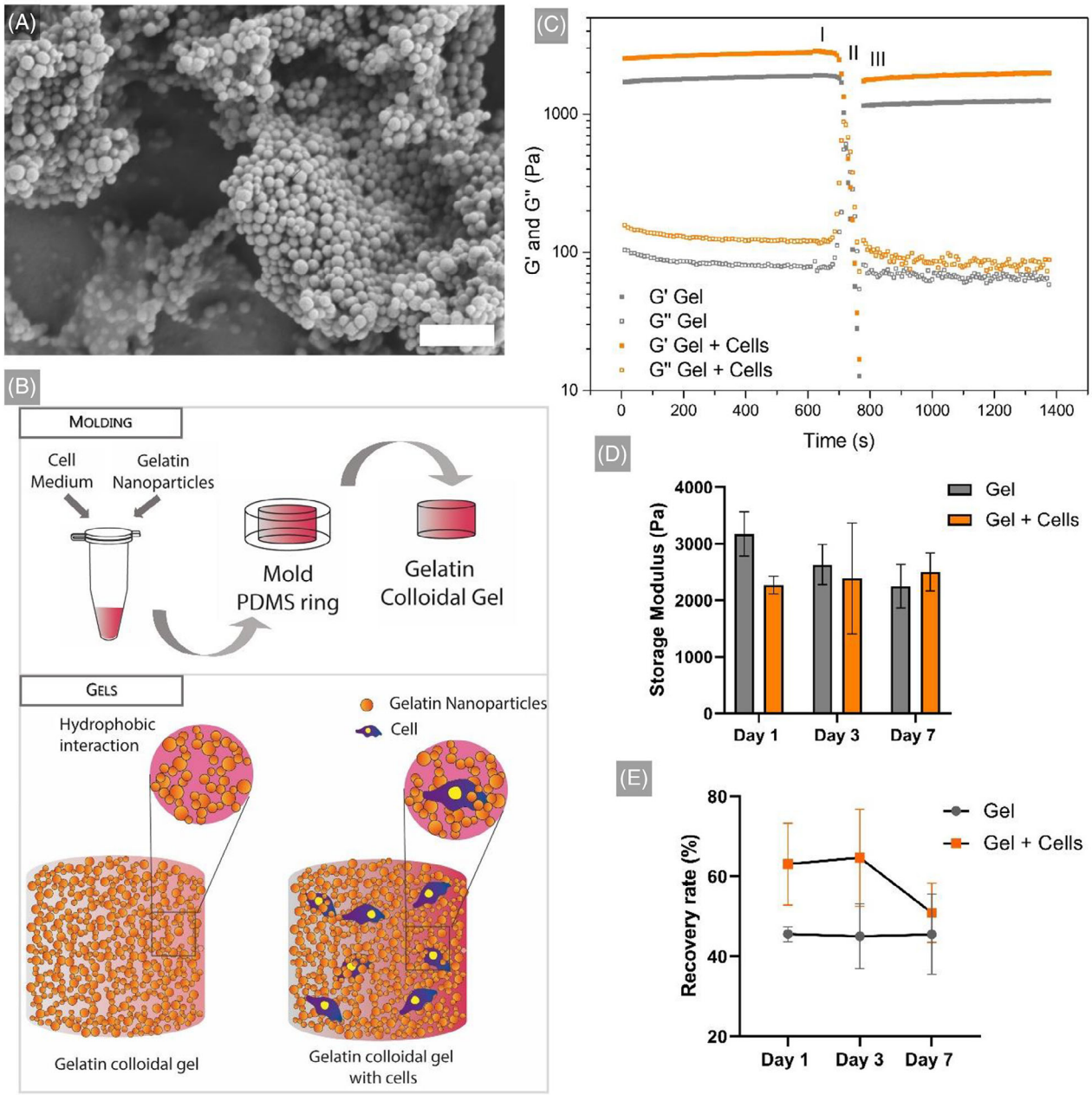

FIGURE 1 (A) Scanning electron microscopy of morphology of gelatin nanoparticles (GNPs) (scale bar represents 1 μm). (B) Schematic representation of the formation of cell-laden gelatin colloidal gels, the molding process and a representation of gelatin colloidal gels and the inclusion of cells in these systems. (C) Representative graphic of the evaluation of self-healing capacity of gelatin colloidal gels before (phase I), during (phase II) and after (phase III) destructive shearing at 1000% strain. (D) Storage modulus of gelatin colloidal gels with or without cells as a function of cell culturing time. (E) Self-healing capacity of gelatin colloidal gels with or without cells as a function of cell culturing time. All experiments were performed in triplicate ($n = 3$).

(hydrodynamic and dry), surface charge, and morphology. As shown in Figure 1A, GNPs presented a spherical morphology and dry size of 163 ± 17 nm. The hydrodynamic size of GNPs, as determined by dynamic light scattering (DLS), was 322 ± 6 nm with a narrow size distribution as evidenced by their low polydispersity index (PDI) value (0.026). The larger hydrodynamic size of GNPs relative to their dry size was attributed to the highly hydrophilic nature of gelatin. In addition, the resulting GNPs showed an almost neutral net surface charge of 1.32 ± 0.14 mV at pH = 7.4.

2.2 | Gelatin colloidal gel formation with or without cells

The GNPs as prepared using the method described in Section 4.2 were first used to evaluate their gel-forming capacity. These preliminary cell-free tests confirmed that cohesive gels could be formed, which is a crucial prerequisite for long-term in vitro cell culture studies at prolonged incubation times. To produce cell-laden colloidal hydrogels, we developed a novel protocol that enabled the incorporation of cells into

gelatin colloidal (Figure 1B). The first step involved preconditioning dry and sterile GNPs in a medium to allow for full swelling of the nanoparticles, thereby ensuring a favorable microenvironment for optimal cell encapsulation into the colloidal gels. The solid content of the GNPs gels in this initial step was 10 w/v%, yielding a gel that displayed elastic, solid-like behavior.[26]

Encapsulation of cells into colloidal gels requires a careful combinatorial approach to optimize various design parameters which affect the biofunctionality of the final cell-laden system. For instance, low cell concentrations typically result in enhanced cell survival and proliferation, but are not relevant for in vivo applications, whereas high cell concentrations can lead to cell oversaturation and hypoxia, which ultimately result in failure of the cell-laden construct.[27] To determine the most appropriate cell concentration for our gelatin colloidal gels, we evaluated the storage modulus and self-healing capacity of gelatin colloidal gels containing three different cell concentrations (0.5, 1, and 2×10^6 cells mL^{-1}). As shown in Figure S1, both storage moduli and self-healing properties of the gelatin colloidal gels did not depend on the cell concentrations. Therefore, we selected the highest cell concentration (i.e., 2×10^6 cells mL^{-1} of gel) for further investigations of the cellular response upon encapsulation of stem cells inside gelatin colloidal gels. No significant differences were observed between the storage modulus (gels with cells: 2.61 ± 0.15 kPa vs. gels without cells: 2.36 ± 0.50 kPa) and self-healing capacity (gel with cells: $59 \pm 3\%$ vs. gel without cells: $57 \pm 3\%$) of gels with or without cells (Figure 1C). These results indicate that the encapsulation of cells did not negatively affect the mechanical properties in the resulting cell-laden system.

2.3 | Cell encapsulation in gelatin colloidal gels

Cellular processes such as migration and proliferation can induce local deformations in the gels by exerting stresses ranging from 0.1 to 10 kPa.[12] Therefore, to investigate how the encapsulated cells interacted with their surrounding microenvironment and affected the viscoelastic properties of gels during long-term cell culture, rheological analysis was conducted over a period of up to 7 days post-encapsulation. As shown in Figure 1D the storage modulus of cell-laden gels did not significantly change over 7 days and remained constant in the range between 2 and 3 kPa. Although the absolute values showed a considerable decrease in the self-healing capacity of gels with cells after 7 days of cell culture (from 60% to 40%), these values were not statistically significant (Figure 1E). Since colloidal gels composed of chemically crosslinked GNPs hardly degrade in vitro, these colloidal gels preserved their integrity over longer time periods, thereby allowing cells to reorganize themselves within the gels.

Live/Dead staining revealed that encapsulated cells were viable during the entire culturing period of 7 days and dead cells were hardly observed (Figure 2A,B). To evaluate the functionality of encapsulated cells within the gels, we performed an AlamarBlue assay to measure their metabolic activity and quantified cell proliferation by analyzing the total DNA content after culturing for up to 7 days. The metabolic activity of the encapsulated cells continuously increased over 7 days of culture (Figure 2C). Moreover, the total amount of DNA at day 7 was statistically higher than day 3, but statistically similar to day 1 (Figure 2D).

Wang et al. previously developed an injectable gel containing cells and assessed their viability in vitro and in vivo.[17] However, in their in vitro study, the cells were seeded on top of gels of different solid content to identify the optimal formulation for cell-laden gels. In their study, mesenchymal stem cells demonstrated proliferation starting from day 4, which further increased with higher gelatin solid content. In contrast, our study did not observe an increase in cell proliferation, although these cells became metabolically more active in our gels over the course of 7 days. These contrasting results may be attributed to the changes in cell behavior caused by their encapsulation inside a 3D system.

Generally, it should be mentioned here that the majority of cell viability studies[17,19,20] on gelatin colloidal gels seeded cells on top of the gels. This method creates a similar environment to a 2D substrate where cells adhere and proliferate rather quickly without facing spatial restrictions characteristic for 3D cell cultures, such as limited access to nutrients and oxygen and stiff extracellular matrices which decelerate cell migration. As a result, the outcomes of currently available cell culture studies on colloidal gels are not directly comparable to our study, which specifically focused on the encapsulation of cells within the colloidal gel matrix.

Our study focused on the encapsulation of cells within a 3D gelatin colloidal gel system, which comes along with a broad range of factors that can influence cell behavior. These factors include the selection of material, mechanical properties of the gels, the encapsulation method, nutrient and oxygen availability, gel porosity, and the ability of cells to remodel their microenvironment. These factors can potentially affect cell functions such as their migration, proliferation, or viability. For instance, when comparing cells seeded on top of 10% GelMA gels to cells encapsulated in similar gels, it was observed that the seeded cells were able to proliferate and survive over 7 days[28] In contrast, the encapsulated cells showed continuous survival but decreased viability at longer incubation times.[29]

The spatial distribution and morphology of cells encapsulated in the gelatin colloidal gels were further studied through histological analysis and confocal microscopy. Histological sections were mainly used to analyze the spatial distribution of encapsulated cells, whereas confocal microscopy allowed to analyze the morphology of encapsulated cells at higher resolution. F-actin staining was used to visualize the cytoskeleton of stem cells (as a measure for cell spreading) embedded within the colloidal gel after 7 days of culture. Histological analysis and confocal imaging (Figure 3) confirmed that the encapsulated stem cells were homogeneously distributed throughout the entire gel, while the stem cells adopted a more spread-out morphology compared to day 1 as observed using both imaging techniques. Immunofluorescence imaging of actin suggested that cell migration may have occurred, as the cell distribution displayed heterogeneity characterized by cell-rich and cell-poor areas (Figure S2).

Based on the above-described results it can be concluded that the protocol presented herein allows to fabricate cell-laden gelatin

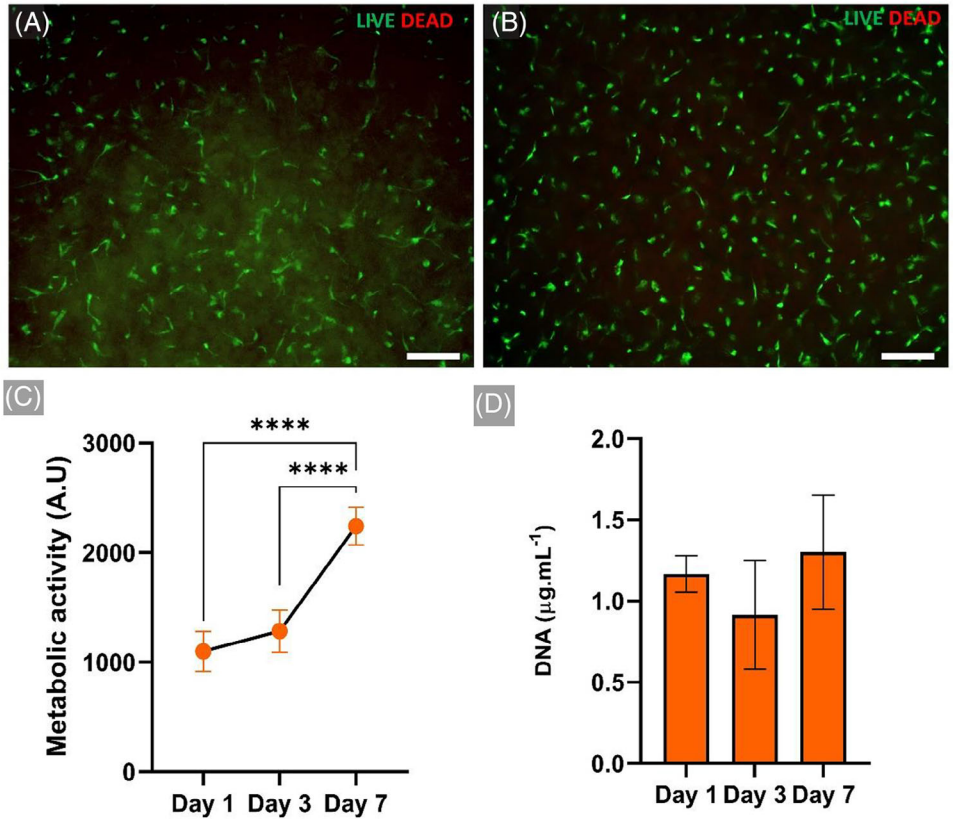

FIGURE 2 Live/Dead assay of cell-laden gelatin colloidal gels containing cells (live cells are displayed in green, dead cells are displayed in red, scale bar corresponds to 200 µm) of day 1 (A) and day 7 (B). (C) Metabolic activity of cells encapsulated in gelatin colloidal gels. (D) Proliferation of cells encapsulated in gelatin colloidal gels. Statistical significances are represented by asterisks (****corresponds to $p < 0.0001$), with $n = 4$.

colloidal gels containing homogeneously dispersed gels. Initial rheological properties were not negatively affected by the cell encapsulation, while 3D-encapsulated cells adopted a spread morphology reminiscent of 2D-cultured adherent cells and more heterogeneous spatial distribution after 7 days of culture. This spreading and migration behavior might have caused the decreased self-healing capacity of cell-laden gels after 7 days of culture (Figure 1E), since the resulting local areas of high cell density and low particle density did not contribute to the self-healing of gelatin colloidal gels enabled by reversible interparticle bonds. Overall, our results showed that encapsulation of cells in gelatin colloidal gels ensures their viability, metabolic activity, and proliferation for up to 7 days of culturing.

To evaluate if the cell-laden gel presented above can indeed act as a delivery vehicle for cells, a simple extrusion assay was performed. The results demonstrated that cells retain their viability after extrusion through narrow needles (25 G), although the cell concentration decreased upon gel extrusion (Figure S3). This reduction in cell concentration can most likely be explained by filter-pressing since the extrusion of the cell-laden gel was accompanied by the initial extrusion of an aqueous phase of lower viscosity.[30] Although cell viability was not negatively affected by gel extrusion, the reliability of bioinks and cell delivery system can be compromised by filter-pressing.[31] In future work, the influence of filter pressing on cell delivery should be investigated by fine-tuning the stability of the colloidal networks, for example, by varying the concentration, size, and charge of the GNPs to minimize filter pressing.[26,31] Our findings showcase that the gelatin colloidal gels can be effectively used as cell delivery vehicles without compromising the initial viscoelastic properties of these colloidal gels. The cell-encapsulated method described herein was simple and straightforward without the need for any crosslinking during/after cell encapsulation, resulting in a homogeneous distribution of cells throughout the gel matrix.

2.4 | Encapsulation of cells partially coated with silica in gelatin colloidal gels

Numerous studies have already shown that the mechanical properties of hydrogels can be improved by the incorporation of inorganic (nano)particles, which typically enhance the stiffness of the resulting composite hydrogels.[19,20,32]

Typically, increasing the stiffness of hydrogels can promote osteogenic and chondrogenic differentiation, yet it may also negatively impact other cellular functions.[15] Recent findings indicate a reduction in the formation of endothelial cell networks within gelatin colloidal gels as stiffness increases.[18] This decrease could be attributed to the higher solid content, potentially altering the properties of gel by reducing self-healing ability and reducing network dynamicity. While

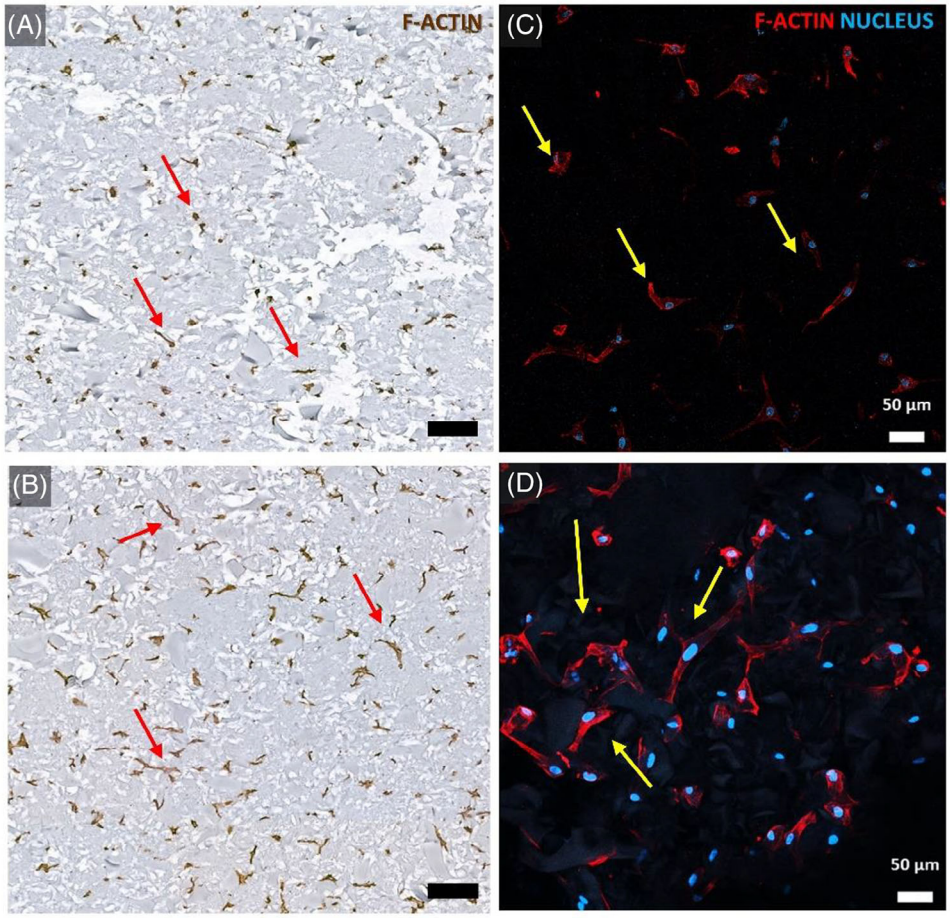

FIGURE 3 F-actin staining using histology of cells cultured for 1 (A) and 7 (B) days in gelatin colloidal gels (scale bar corresponds to 100 µm). F-actin (brown) and gelatin colloidal gel (gray). Red arrows point to actin filaments of cells showing the difference in elongation between day 1 and day 7. F-actin staining using immunofluorescence of cells cultured for 1 (C) and 7 (D) days in gelatin colloidal gels (scale bar corresponds to 50 µm). F-actin (red), nucleus (blue). Yellow arrows point to the actin filament of cells.

incorporating additional building blocks may successfully enhance the mechanical properties of colloidal gels, the processes required for such incorporation(e.g. high-speed centrifugation) can also negatively affect cell survival. Therefore, we explored the feasibility of encapsulating cells with protective inorganic coatings to enhance the overall mechanical integrity of the resulting cell-laden system.

To this end, we prepared human-derived adipose mesenchymal stem cells partially covered with a silica layer (SiCells). These cells were previously shown to be protected by these coatings when cultured in suspension, without any available surface to adhere.[24] The encapsulation of cells partially coated with silica in gelatin colloidal gels (Gels + SiCells) resulted in a doubling of storage modulus after day 7 (Figure 4A) (day 1: 1.38 ± 0.67 kPa vs. day 7: 3.85 ± 0.19 kPa), while the self-healing capacity of the resulting cell-laden gels also dropped after 7 days to about 40% in a manner similar to silica-free cell-laden gels (Figure 4B). Live/Dead assay showed that cells were viable inside the gelatin colloidal gels by day 1 (Figure 4C) and day 7 (Figure 4D). Cell metabolic activity increased significantly from day 3 to day 7, while the total amount of DNA showed a slightly increasing trend, but the differences between various time points were not statistically significant (Figure 4E,F, respectively). The absolute values for metabolic activity and cell proliferation were lower in comparison to silica-free systems, which could be caused by the silica interaction with the different assays and/or an initial lower number of encapsulated cells partially coated with silica. F-actin staining in both histological sections (Figure 4G,H and Figure S4), as well as immunofluorescence images (Figure 4I,J), show that cells were spatially distributed and spread out in a manner similar to silica-free cell-laden gels, thereby confirming that the silica coatings did not negatively affect cell distribution and spreading.

In vitro studies of cell-laden gels are crucial to understanding differences in cell behavior when cultured inside or on top of gels. Generally, cell confinement by surrounding materials can induce contrasting results compared to cells seeded on top of materials, depending on a variety of factors such as the physicochemical properties of the biomaterial itself, the specific cell type, or the intended application. Although encapsulation of cells in gelatin colloidal systems was recently achieved,[17,18] the behavior of cells in these systems is still poorly understood. In this work, we encapsulate cells both pristine and modified in gelatin colloidal systems in an effective and simple manner with cells achieving a homogeneous distribution throughout the

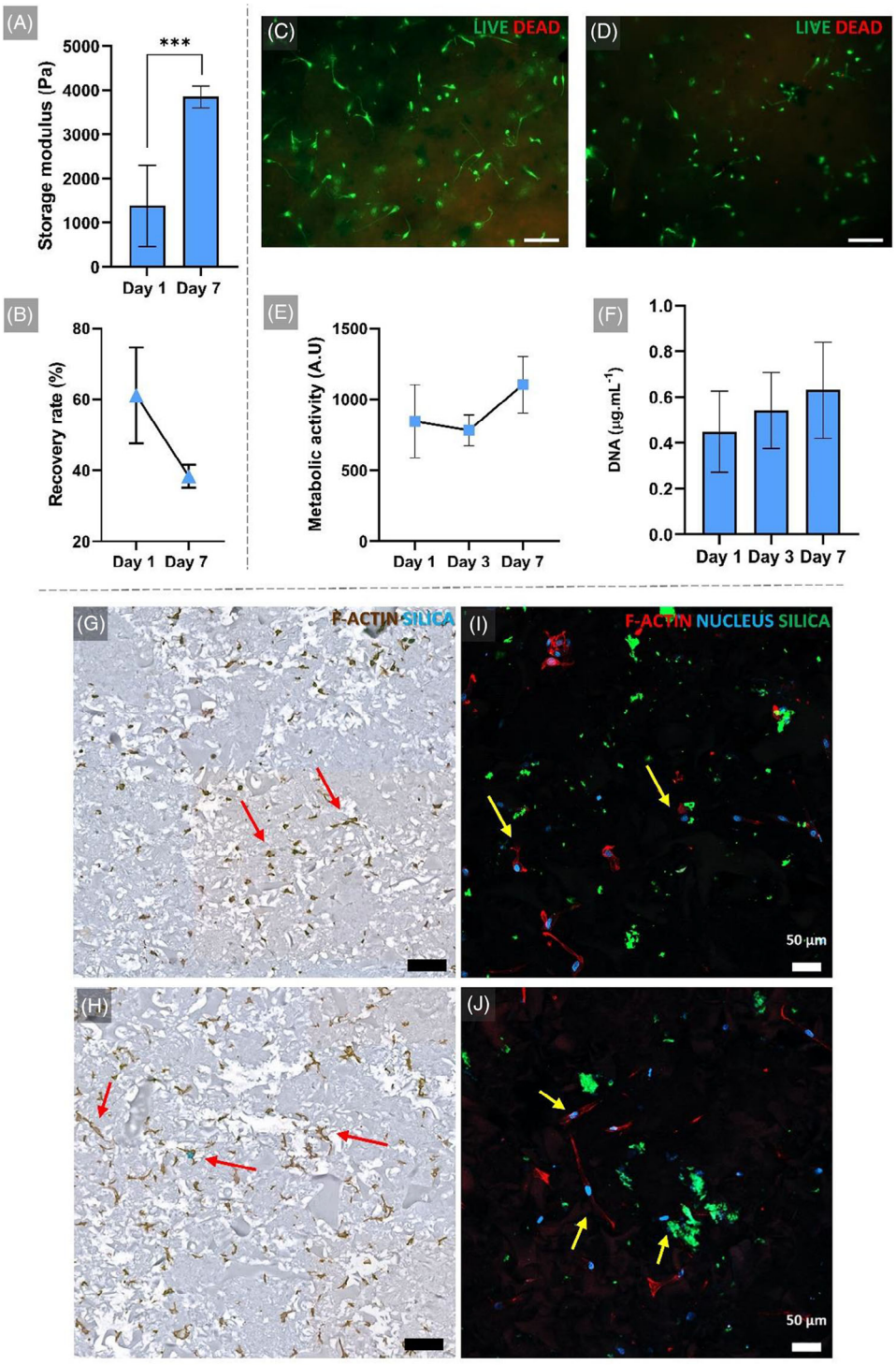

FIGURE 4 (A) Storage modulus of gelatin colloidal gels containing cells partially coated with silica as a function of cell culturing time. (B) Self-healing capacity of gelatin colloidal gels with cells partially coated with silica as a function of cell culturing time. Statistical significance with *** with $p = 0.0002$, $n = 3$; Live/Dead assay of cell-laden gelatin colloidal gels (live cells are displayed in green, dead cells are displayed in red, scale bar corresponds to 200 µm) of day 1 (C) and day 7 (D). (E) Metabolic activity and (F) DNA quantification of silica-coated cells encapsulated in gelatin colloidal gels $n = 4$; F-actin staining using histology of cells partially coated with silica cultured for 1 (G) and 7 (H) days in gelatin colloidal gels (scale bar corresponds to 100 µm). F-actin (brown), gelatin colloidal gel (gray), and silica (blue). Red arrows point to actin filaments of cells showing the difference in spreading between day 1 and day 7. F-actin staining using immunofluorescence of cells cultured for 1 (I) and 7 (J) days in gelatin colloidal gels (scale bar corresponds to 50 µm). F-actin (red), nucleus (blue), and silica (green). Yellow arrows point to the actin filament of cells.

gel. Cell-laden gels were cohesive after cell inclusion, which is crucial for applications like bioprinting, although their self-healing capacity reduced with increasing cell culturing time. Compared to gels loaded with pristine cells, the encapsulation of cells partially coated with silica enhanced the storage modulus of the resulting cell-laden gels after 7 days in culture. During these 7 days of culture, cells were able to adapt and spread inside the gels, which boosted their metabolic activity although proliferation remained stable. We attribute this delayed mechanical reinforcement of colloidal gels using cells partially coated with silica to spreading of these cells over time, thereby expanding their interaction area with the surrounding matrix. Initially, the local effects of silica coating did not significantly impact the overall mechanical properties of hydrogels, stressing that the mere addition of silica to the colloidal gel did not automatically result in reinforcement of these cell-laden colloidal gels. However, after 7 days, these cell-laden gels behave differently from a mechanical perspective, as cells reorganize within the gel. These cells partially coated with silica act as fillers, temporally modulating mechanical properties – an important factor given the direct responsiveness of cells to the stiffness of the surrounding matrix.[18] Apparently, the cells partially coated with silica induced a reinforcing mechanism with prolonged cell culturing time, which we attribute to enhanced physico-chemical interaction between the silica-coated cells and the surrounding colloidal gel matrix, thereby increasing the resistance of the cell-laden gels to mechanical deformation. As such, the silica-coated cells enhanced the cohesion of the gels by a cellular crosslinking mechanism. Future studies should focus on devising protocols that explore cell-material interactions and hydrogel properties across different scales of deformation. The mechanics of hydrogels appear to vary with deformation mode and scale, emphasizing the need to introduce cells early and comprehend their evolving behavior over time.[33]

Importantly, our cellular gel reinforcing strategy avoids additional incorporation of separate inorganic particles that inevitably increase the complexity of the system, which could negatively affect cell viability. These cells partially coated with silica can be used as fillers or cell-protecting agents during extrusion through narrow syringes but also to functionalize silica with different molecules or functional groups to facilitate drug delivery applications or biochemically modulate the behavior of cells.[34]

Overall, cell-laden colloidal gels offer a promising alternative to commonly used bioink systems and other cell culture matrices without requiring post-treatments like potentially toxic chemical cross-linking. Due to their much smaller particle size than microgels, nanogels (as building blocks for colloidal gels) exhibit a higher specific surface area, which allows for (i) more interaction with cells at the nanoscale and (ii) formation of more cohesive colloidal gels as compared to gels composed of larger microgels.[31] Additionally, the ability to functionalize different building blocks allows to adjust the mechanical properties of the system according to the functional characteristics of the ECM of different human tissues, which underlines the strong potential of these systems for areas such as tissue engineering, regenerative medicine, and development of advanced disease models. However, a knowledge gap in fundamental understanding of cell-material interactions still exists for these novel biomaterials. Therefore, long-term in vitro and in vivo studies should be performed to enhance our understanding of cellular behavior as a function of the viscoelastic properties of these systems depending on parameters such as gelatin solid content or nanoparticle surface charge. In addition, future studies should be conducted on the bioprinting ability of this colloidal gel system to unleash their potential for tissue engineering and cell delivery applications.

3 | CONCLUSION

In conclusion, this study confirms the strong potential of gelatin colloidal gels as a promising solution to solve challenges in cell delivery and biofabrication. The attractive self-healing and viscoelastic properties of these gels facilitate successful encapsulation of viable and metabolically active stem cells. By encapsulation of stem cells within gelatin colloidal gels, we achieved a homogeneous distribution of cells throughout the gel matrix and conducted a comprehensive evaluation of their cellular behavior and their effect on the viscoelastic properties of the resulting cell-laden gels. The encapsulated cells demonstrated high viability and seamlessly adapted to the gel matrix without significant alterations to their viscoelastic properties. Furthermore, the incorporation of cells partially coated with silica into the gel structure resulted in increased stiffness after 7 days of culture. These cells partially coated with silica offer an innovative approach to modulate the functional properties of colloidal gels, without the need to incorporate additional inorganic reinforcing particles. As such, these cells partially coated with silica hold potential as fillers to modulate the mechanical properties of cell-laden gels. Moreover, the opportunity to functionalize these silica coatings with various biomolecules or functional groups creates exciting new prospects for drug delivery applications and cell modulation. In summary, this study contributes to our understanding of cell-material interactions within 3D colloidal gels, thereby contributing to the advancement and practical application of colloidal gels in biomedicine.

4 | EXPERIMENTAL SECTION

4.1 | Materials

Gelatin type A (Bloom number 285) was kindly provided by Rousselot (Ghent, Belgium). Glutaraldehyde (25 wt% aqueous solution) was purchased from Acros. Tetraethyl orthosilicate (TEOS, reagent grade, 98%), fluorescein isothiocyanate (FITC), Alcian Blue 8GX certified biological stain (AB), hydrochloric acid 37% (HCl), N-2-hydroxyethylpiperazine-N'−2-ethanesulfonic acid (HEPES), hematoxylin, eosin, formaldehyde, and PBS were purchased from Merck. (3-Aminopropyl) triethoxysilane (APTES, 99%) was acquired from Enzymatic S.A. Dulbecco's phosphate-buffered saline (DPBS) powder without calcium/magnesium for cell culture was obtained from Corning. Ethanol absolute (EtOH) and acetone were acquired from Boom. All other chemicals were reagent grade and used without any purification.

4.2 | Gelatin nanoparticle synthesis

GNPs were produced by a two-step desolvation method which was previously described in detail.[35,36] The first desolvation step was applied to remove low molecular weight gelatin. Briefly, 25 g of gelatin was dissolved in 500 mL of demineralized water (dH_2O) under stirring (500 rpm) at 50°C. Then, 500 mL of acetone was rapidly added to the gelatin solution under vigorous stirring (1000 rpm). After 3 min, the mixture was left at room temperature (RT) for 15 min to precipitate the high-molecular-weight gelatin. The supernatant was then discarded, and the remaining high molecular weight gelatin was dissolved in 450 mL of demineralized water and freeze-dried for 48 h. For the second step of desolvation, 2.5 g of the freeze-dried gelatin was dissolved in 50 mL of dH_2O. Subsequently, the pH of the solution was adjusted to 2.5 using hydrochloric acid (6 M). Afterward, 120 mL of acetone was added dropwise at an injection rate of 8.0 mL min^{-1} under stirring (1000 rpm) at 40°C. To stabilize the GNPs, 316 µL of glutaraldehyde solution was added and left overnight under stirring at RT. The nanoparticle crosslinking reaction was stopped by adding 100 mL of glycine (100 mM) under stirring for 30 min. Afterward, the GNPs were collected by centrifugation (16,800 rcf, 40 min) and washed three times by redispersion in dH_2O. The collected GNPs were dispersed in an acetone/water mixture (30/70 v/v%), frozen with liquid nitrogen, and freeze-dried for 3 days.

4.3 | Gelatin nanoparticle characterization

The hydrodynamic diameter of GNPs dispersed in water was determined by DLS using a Malvern Zetasizer Nano-Z at 25°C, setting a minimum of 10 and a maximum of 100 runs per measurement. The zeta potential of GNPs was determined using the same instrument by means of laser doppler velocimetry. The GNPs were collected after washing and redispersed in 5 mM HEPES buffer (pH 7.4). The nanoparticle morphology and size in dry state were studied using a Field Emission Scanning Electron Microscope (FE-SEM; Sigma 300, Zeiss, Germany). Dried nanoparticles were placed on a double-stick carbon tape followed by coating with an electroconductive chromium layer with a thickness of around 10 nm. The average size and size distribution of nanoparticles were determined by measuring the diameter of at least 100 particles using ImageJ software.

4.4 | Cell culture

Human adipose mesenchymal stem cells (hASCs, passages between P6 and P7) were isolated from subcutaneous adipose tissue obtained by liposuction, following informed consent and patient anonymization, according to good practices standards. The retrieval and transportation of the samples to the laboratory facilities were performed under a cooperation agreement between Compass Research Group and Hospital da Luz of Aveiro, after approval of the Competent Ethics Committee (CEC), handled by the guidelines approved by the CEC. hASCs were cultured in 175 cm^2 T-flasks with α-MEM supplemented with sodium bicarbonate, 10 v/v% fetal bovine serum (FBS), and 1 v/v% antibiotic (penicillin/streptomycin) (α-MEM) at 37°C under a humidified air atmosphere of 5% CO_2. Cells were detached at 80% of confluency using trypsin-EDTA (Thermo Fischer Scientific) treatment for 5 min at 37°C.

4.5 | Partial silica coating of hASCs

The protocol to partially coat hASCs with silica was described in a previous report.[24] hASCs were seeded in a tissue culture dish (Ø 100 mm, Sarstedt) with a cell density of 1×10^6 cells per dish. To produce the silica layer, the cell medium was discarded, and hASCs were washed with α-MEM FBS-free with 1% antibiotic. The protocol to achieve a partial coating in the part of the cell membrane consists in two main steps, first the primer step and then the silicification step. In the primer step, 5 mL of 0.5 mg mL^{-1} chitosan-carnitine (CHT-CAR) in PBS (previously heated at 37°C) was added to each culture dish. After 10 min of incubation at 37°C, 5% of CO_2, the CHT-CAR solution was discarded and another washing step with FBS-free α-MEM was performed.

Prior to the silicification step, 1 M of TEOS was hydrolyzed in 1 mM of aqueous HCl solution for 24 h under magnetic stirring at 30°C. 1 M of APTES was hydrolyzed in 1 mM of aqueous HCl solution at RT under magnetic stirring for 24 h. APTES was diluted in a 1:1 ratio of ethanol (EtOH) with other reagents for specific assays. FITC (1 mg mL^{-1} in EtOH) was used for immunofluorescence assays and Alcian Blue (AB, 1 mg mL^{-1} in EtOH) was used for cell integrity assays, rheology, viability, and histology. In the silicification step, the following solution was prepared for each tissue-cultured dish: 4.75 mL FBS-free α-MEM, 62.5 µL of TEOS, and 187.5 µL of APTES. The solution was left to incubate for 20 min at 37°C, 5% of CO_2, and then discarded. Subsequently, hASCs were washed twice with FBS-free α-MEM and then supplemented α-MEM was added to incubate the cells until further use.

4.6 | Preparation of gelatin colloidal gels

A predetermined amount of GNPs was subjected to UV-light sterilization for 30 min. Gelatin colloidal gels were prepared by dispersing 20 mg of freeze-dried GNPs in 2 mL of α-MEM whereafter the gels were left overnight in a 2 mL Eppendorf tube at 4°C. Then, the mixture was centrifuged (12,000 rcf, 10 min) to remove the excess medium, obtaining a homogeneous 10 w/v% hydrogel. For cell encapsulation in gelatin colloidal gels, first cells were harvested and added to Eppendorf tubes at three different cell concentrations, that is, 0.5, 1 and 2×10^6 cells mL^{-1}. These cell suspensions were then concentrated in 50 µL of α-MEM, added to the 10 w/v% gelatin colloidal gel, and thoroughly mixed with a pipet tip and 5 s of vortexing at high speed, yielding a final solid gelatin content of the resulting cell-laden gelatin colloidal gels of 8 w/v%. To ensure the production of gels with same size and shape for the various assays, we mold the gels in polydimethylsiloxane (PDMS) rings. Acellular controls were prepared following the same procedure

but without adding cells. Gels were left at 37°C in a water bath until further use.

4.7 | Rheological analysis

For rheological analysis, the viscoelastic parameters of gelatin colloidal gels with or without cells were assessed 4 h as well as 1, 3, and 7 days after cell encapsulation. Briefly, gels were transferred into PDMS rings and then incubated in α-MEM, under 5% CO_2 at 37°C. Then, the gels were transferred to the Peltier plate of the rheometer without the PDMS rings previous to each measure. Rheological properties of colloidal gels were evaluated using an AR2000 Advanced Rheometer (TA Instruments) with a flat steel plate geometry (8 mm diameter) at a gap distance of 500 μm at 37°C. To avoid evaporation during measurements, the geometry was sealed with silicon oil. Time sweeps (5 min at 0.5% strain and an oscillatory frequency of 1 Hz) were performed to determine the storage modulus (G') and loss modulus (G'') of both cell-free and cell-laden gelatin colloidal gels. The self-healing capacity of these gels was defined as their ability to recover from mechanical damage (e.g. by applying destructive shearing). For this purpose, three consecutive steps were performed including a time sweep for 1 min at 0.5% strain and a frequency of 1 Hz, (i) a strain sweep from 0.1% to 1000% strain at a frequency of 1 Hz and (ii) a time sweep for 5 min at 0.5% strain and a frequency of 1 Hz. The self-healing capacity of the gels was subsequently quantified by dividing the recovery (%) of the storage modulus (G') of the gels after the strain sweep relative to their initial G' prior to the strain sweep. All experiments were performed in triplicate ($n = 3$).

4.8 | Biochemical assays for cellular metabolic activity, viability, and proliferation

All biochemical assays were performed at predetermined time points of 1, 3, and 7 days after cell encapsulation for both cell-free controls and cell-laden gels ($n = 4$). Sample preparation was performed as described in Section 4.6 and molded in PDMS rings with a diameter of 4 mm and a height of 2 mm. To evaluate the viability of encapsulated cells, cell-laden gels were transferred into an Ibidi 8-well plate and incubated at 37°C under a humidified air atmosphere of 5% CO_2. Live/Dead staining was performed after incubation of cell-laden gels and controls in a mixture of 4 μL of Calcein AM (1 mg mL^{-1}) and 2 μL of propidium iodide (PI) (1 mg.mL^{-1}) in 1 mL of PBS at 37°C for 40 min protected from light. Afterward, the different gels were analyzed using fluoresce microscopy using an Axio Imager 2 (Zeiss, Germany), and the acquired images were further processed in Zeiss Zen Blue software. For quantification of cellular metabolic activity, cell-laden gels were kept in 48 well-plates in an incubator at 37°C, 95% relative humidity under a humidified air atmosphere containing 5% CO_2. At each time point (day 1, 3, 7), the culture medium was removed, and 400 μL of 10 v/v% AlamarBlue reagent was added and incubated for 6 h at 37°C. Then, the supernatant was transferred into a 96 well-plate, and the fluorescence intensity was measured in a multimodal microplate reader (Gen 5 software, Synergy HTX, BioTek Instrument, USA) with an excitation wavelength of 530/25 nm and emission wavelength of 590/25 nm. Afterward, each well was washed two times with PBS to remove the Alamar blue reagent whereafter 400 μL of fresh media was added and the plate was incubated until the next time point. Gels without cells were considered as blanks, and their fluorescent intensity was subtracted from the experimental samples. Total dsDNA quantification was performed as a measure of cellular proliferation using the assay kit Quant-iT PicoGreen (Life Technologies). Cell-laden gels were prepared as described in Section 4.6 and then transferred into 48-well plates. At each time interval (days 1, 3, and 7), the medium was removed, and gels were washed with dPBS and transferred into 1.5 mL Eppendorf tubes. Samples were frozen at −80°C at least overnight. To digest the gelatin-based colloidal gels, 500 μL of proteinase K (100 μg mL^{-1} in 50 mM Tris-HCl and 3 mM CaCl2, pH = 7.8) was added to each Eppendorf containing samples followed by mixing in a ThermoMixer C (Eppendorf) for 30 min (56°C, 1000 rpm). After complete digestion, the DNA content of gels was quantified as a measure of cellular proliferation according to the specifications of the assay kit. A standard curve for DNA analysis was generated using the provided dsDNA solution. After 10 min of incubation at RT, the fluorescent intensity of the samples was measured at an excitation wavelength of 485/20 nm and emission wavelength of 528/20 nm using a microplate reader (Gen 5 software, Synergy HTX, Biotek Instruments, USA).

4.9 | Histological analysis

Histological analysis of cell-laden gelatin colloidal gels was performed to evaluate the distribution and morphology of the cells inside the colloidal gels at different time points. Cell-laden colloidal gels were retrieved after 1, 3, and 7 days of culture, subsequently fixed in 4% formaldehyde in PBS for 24 h at temperature, and further processed in a tissue processor (TP1020, Leica). After paraffin embedding, samples were cut into 5 mm sections using a microtome (RM2165, Leica). Sections were melted to microscopy slides (Thermo Fisher Scientific), deparaffinized, and rehydrated before staining. To check the presence of actin filaments in the structure, different sections of histological samples were processed for actin staining. Briefly, after the deparaffinization process, endogenous peroxidases were inactivated with hydrogen peroxide (H_2O_2, 3% v/v in methanol) for 20 min, followed by antigen retrieval using sodium citrate buffer (pH = 6.0) heated up to 70°C for 10 min. After cooling down until 37°C, non-specific binding was blocked with normal donkey serum (NDS, 10% v/v in PBS with glycine for 20 min). The sections were incubated with mouse monoclonal beta-Actin (MoAB-Actin, ab6276 from Abcam, 1:8000 in 2% v/v NDS) and incubated at 4°C overnight. The second antibody (DaMBio 1:5000 in 2% NDS with glycine) was added for 1 h at RT, and the stain was revealed with a 3, 3′-diaminobenzidine (DAB) solution. Afterward, the sections were counterstained with hematoxylin and mounted in Dibutylphthalate Polystyrene Xylene (DPX), a mounting medium to preserve before microscopic analysis. All histological slides were

scanned using the Pannoramic 1000 digitalization system at 20× magnification, and the images were processed using CaseViewer software version 2.3 (3DHISTECH,).

4.10 | Cytoskeletal F-Actin imaging

Samples were collected after 1, 3, and 7 days of culture, and subsequently fixed with 4% formaldehyde in PBS at RT for 2 h. After thorough washing with PBS, these samples were stained with 1:100 Flash Phalloidin FITC (Biolegend): PBS for 1 h at RT followed by staining with 1:1000 DAPI (1 mg mL^{-1}, Thermo Fischer): PBS for 30 min at RT. Samples were visualized by laser confocal scanning microscopy (LCSM) (LSM 900, Carl Zeiss, Germany) and the acquired images were further analyzed using Zeiss Zen Blue software.

4.11 | Gel extrusion assay

Cell-laden gels were prepared according to the method described in Section 4.6, and subsequently loaded into a 1 mL syringe tube using a spatula. Then, using a 1 mL syringe equipped with a 25 G needle and using a flow rate of 20 $mL.h^{-1}$, cell-laden gelatin colloidal gels were extruded and incubated with Live/Dead solution for 30 min at 37°C. The viability was then assessed through fluorescence microscopy using an Axio Imager 2 (Zeiss, Germany), and the acquired images were further processed in Zeiss Zen Blue software.

4.12 | Statistical analysis

Statistical analysis was carried out by performing a Two-way ANOVA followed by a Tukey post hoc test (GraphPad Prism v6.0). The results are presented as average ± standard deviation for rheological assays ($n = 3$) and biological assays ($n = 4$). A p-value < 0.05 was interpreted as statistically significant and indicated with an asterisk symbol in the figures (*).

AUTHOR CONTRIBUTIONS

Marta M. Maciel: Conceptualization; data curation; formal analysis; investigation; methodology; visualization; writing – original draft; and writing – review & editing. Negar Hassani Besheli: Conceptualization; data curation; formal analysis; methodology; writing – original draft; and writing – review & editing. Tiago R. Correia: Methodology; validation; and writing – review & editing. João F. Mano: Conceptualization; Funding acquisition; methodology; project administration; supervision; and writing – review & editing. Sander C. G. Leeuwenburgh: Conceptualization; funding acquisition; methodology; project administration; supervision; and writing – review & editing.

ACKNOWLEDGMENTS

The authors would like to acknowledge the financial support from FCT through the PhD grant (PD/BD/139117/2018 & COVID/BD/152645/2022) (Marta M. Maciel) and a Junior Researcher Grant of the Radboud Institute for Molecular Life Science (RIMLS) of Radboudumc (Negar Hassani Besheli).

CONFLICT OF INTEREST STATEMENT

The authors declare no conflict of interest.

DATA AVAILABILITY STATEMENT

Data available on request from the authors.

ORCID

Sander C. G. Leeuwenburgh https://orcid.org/0000-0003-1471-6133

REFERENCES

1. Khademhosseini, A., & Langer, R. (2016). A decade of progress in tissue engineering. *Nature Protocols*, *11*, 1775–1781.
2. Correia, C. R., Bjørge, I. M., Nadine, S., & Mano, J. F. (2021). Minimalist tissue engineering approaches using low material-based bioengineered systems. *Advanced Healthcare Materials*, *10*, 1.
3. Correa, S., Grosskopf, A. K., Lopez Hernandez, H., Chan, D., Yu, A. C., Stapleton, L. M., & Appel, E. A. (2021). Translational applications of hydrogels. *Chemical Reviews*, *121*, 11385.
4. Li, J., Wu, C., Chu, P. K., & Gelinsky, M. (2020). 3D printing of hydrogels: Rational design strategies and emerging biomedical applications. *Materials Science and Engineering: R: Reports*, *140*, 100543.
5. Bakht, S. M., Pardo, A., Gómez-Florit, M., Reis, R. L., Domingues, R. M. A., & Gomes, M. E. (2021). Engineering next-generation bioinks with nanoparticles: Moving from reinforcement fillers to multifunctional nanoelements. *Journal of Materials Chemistry B*, *9*, 5025.
6. Grimaudo, M. A., Krishnakumar, G. S., Giusto, E., Furlani, F., Bassi, G., Rossi, A., Molinari, F., Lista, F., Montesi, M., & Panseri, S. (2022). Bioactive injectable hydrogels for on demand molecule/cell delivery and for tissue regeneration in the central nervous system. *Acta Biomaterialia*, *140*, 88.
7. Groll, J., Burdick, J. A., Cho, D.-W., Derby, B., Gelinsky, M., Heilshorn, S. C., Jüngst, T., Malda, J., Mironov, V. A., Nakayama, K., Ovsianikov, A., Sun, W., Takeuchi, S., Yoo, J. J., & Woodfield, T. B. F. (2018). A definition of bioinks and their distinction from biomaterial inks. *Biofabrication*, *11*, 013001.
8. Blaeser, A., Duarte Campos, D. F., Puster, U., Richtering, W., Stevens, M. M., & Fischer, H. (2016). Controlling shear stress in 3D bioprinting is a key factor to balance printing resolution and stem cell integrity. *Advanced Healthcare Materials*, *5*, 326.
9. Hasturk, O., & Kaplan, D. L. (2019). Cell armor for protection against environmental stress: Advances, challenges and applications in micro- and nanoencapsulation of mammalian cells. *Acta Biomaterialia*, *95*, 3.
10. Schwab, A., Levato, R., D'este, M., Piluso, S., Eglin, D., & Malda, J. (2020). Printability and shape fidelity of bioinks in 3D bioprinting. *Chemical Reviews*, *120*, 11028.
11. Diba, M., Spaans, S., Ning, K., Ippel, B. D., Yang, F., Loomans, B., Dankers, P. Y. W., & Leeuwenburgh, S. C. G. (2018). Self-healing biomaterials: From molecular concepts to clinical applications. *Advanced Materials Interfaces*, *5*, 1.
12. Bertsch, P., Andrée, L., Besheli, N. H., & Leeuwenburgh, S. C. G. (2022). Colloidal hydrogels made of gelatin nanoparticles exhibit fast stress relaxation at strains relevant for cell activity. *Acta Biomaterialia*, *138*, 124.
13. Freitas, B., Lavrador, P., Almeida, R. J., Gaspar, V. M., & Mano, J. F. (2020). Self-assembled bioactive colloidal gels as injectable multiparticle shedding platforms. *ACS Appl Mater Interfaces*, *12*, 31282.

14. Douglas, A. M., Fragkopoulos, A. A., Gaines, M. K., Lyon, L. A., Fernandez-Nieves, A., & Barker, T. H. (2017). Dynamic assembly of ultrasoft colloidal networks enables cell invasion within restrictive fibrillar polymers. *PNAS*, *114*, 885.
15. Lin, M. H., Linares, I., Ramirez, C., Ramirez, Y. C., & Sarkar, D. (2023). Mechanomorphological guidance of colloidal gel regulates cell morphogenesis. *Macromolecular Bioscience*, *23*, 2300122.
16. Su, K., & Wang, C. (2015). Recent advances in the use of gelatin in biomedical research. *Biotechnology Letters*, *37*, 2139.
17. Wang, Y., Zhang, Y., Chen, K., Shao, F., Wu, Y., Guo, C., Wu, H., Zhang, D., Li, W., Kong, Q., & Wang, H. (2021). Injectable nanostructured colloidal gels resembling native nucleus pulposus as carriers of mesenchymal stem cells for the repair of degenerated intervertebral discs. *Materials Science & Engineering, C: Biomimetic and Supramolecular Systems*, *128*, 112343.
18. Nair, S. K., Basu, S., Sen, B., Lin, M. H., Kumar, A. N., Yuan, Y., Cullen, P. J., & Sarkar, D. (2019). Colloidal gels with tunable mechanomorphology regulate endothelial morphogenesis. *Scientific Reports*, *9*, 1.
19. Dou, Z., Tang, H., Chen, K., Li, D., Ying, Q., Mu, Z., An, C., Shao, F., Zhang, Y., Zhang, Y., Bai, H., Zheng, G., Zhang, L., Chen, T., & Wang, H. (2023). Highly elastic and self-healing nanostructured gelatin/clay colloidal gels with osteogenic capacity for minimally invasive and customized bone regeneration. *Biofabrication*, *15*, 025001.
20. Diba, M., Camargo, W. A., Brindisi, M., Farbod, K., Klymov, A., Schmidt, S., Harrington, M. J., Draghi, L., Boccaccini, A. R., Jansen, J. A., Van Den Beucken, J., & Leeuwenburgh, S. C. G. (2017). Composite colloidal gels made of bisphosphonate-functionalized gelatin and bioactive glass particles for regeneration of osteoporotic bone defects. *Advanced Functional Materials*, *27*, 1.
21. Diba, M., Polini, A., Petre, D. G., Zhang, Y., & Leeuwenburgh, S. C. G. (2018). Fiber-reinforced colloidal gels as injectable and moldable biomaterials for regenerative medicine. *Materials Science & Engineering, C: Biomimetic and Supramolecular Systems*, *92*, 143.
22. Zhuang, Z., Sun, S., Chen, K., Zhang, Y., Han, X., Zhang, Y., Sun, K., Cheng, F., Zhang, L., & Wang, H. (2022). Gelatin-Based colloidal versus monolithic gels to regulate macrophage-mediated inflammatory response. *Tissue Eng.—Part C Methods*, *28*, 351.
23. Laschke, M. W., & Menger, M. D. (2017). Life is 3D: Boosting spheroid function for tissue engineering. *Trends Biotechno*, *35*, 133.
24. Maciel, M. M., Correia, T. R., Gaspar, V. M., Rodrigues, J. M. M., Choi, I. S., & Mano, J. F. (2021). Partial coated stem cells with bionspired silica as new generation of cellular hybrid materials. *Advanced Functional Materials*, *31*, 1.
25. Si, Z., Wang, X., Sun, C., Kang, Y., Xu, J., Wang, X., & Hui, Y. (2019). Adipose-derived stem cells: Sources, potency, and implications for regenerative therapies. *Biomedicine & Pharmacotherapy*, *114*, 108765.
26. Wang, H., Hansen, M. B., Löwik, D., Van Hest, J. C. M., Li, Y., Jansen, J. A., & Leeuwenburgh, S. C. G. (2011). Oppositely charged gelatin nanospheres as building blocks for injectable and biodegradable gels. *Advanced Materials*, *23*, 119.
27. Cidonio, G., Glinka, M., Dawson, J. I., & Oreffo, R. O. C. (2019). The cell in the ink: Improving biofabrication by printing stem cells for skeletal regenerative medicine. *Biomaterials*, *209*, 10.
28. Wang, Y., Ma, M., Wang, J., Zhang, W., Lu, W., Gao, Y., Zhang, B., & Guo, Y. (2018). Development of a photo-crosslinking biodegradable GelMA/PEGDA hydrogel for guided bone regeneration materials. *Materials*, *11*, 1345.
29. Krishnamoorthy, S., Noorani, B., & Xu, C. (2019). Effects of encapsulated cells on the physical–mechanical properties and microstructure of gelatin methacrylate hydrogels. *International Journal of Molecular Sciences*, *20*, 5061.
30. Diba, M., Koons, G. L., Bedell, M. L., & Mikos, A. G. (2021). 3D printed colloidal biomaterials based on photo-reactive gelatin nanoparticles. *Biomaterials*, *274*, 120871.
31. Wang, H., Boerman, O. C., Sariibrahimoglu, K., Li, Y., Jansen, J. A., & Leeuwenburgh, S. C. G. (2012). Comparison of micro- vs. nanostructured colloidal gelatin gels for sustained delivery of osteogenic proteins: Bone morphogenetic protein-2 and alkaline phosphatase. *Biomaterials*, *33*, 8695.
32. Zandi, N., Sani, E. S., Mostafavi, E., Ibrahim, D. M., Saleh, B., Shokrgozar, M. A., Tamjid, E., Weiss, P. S., Simchi, A., & Annabi, N. (2021). Nanoengineered shear-thinning and bioprintable hydrogel as a versatile platform for biomedical applications. *Biomaterials*, *267*, 120476.
33. Andrée, L., Bertsch, P., Wang, R., Becker, M., Leijten, J., Fischer, P., Yang, F., & Leeuwenburgh, S. C. G. (2023). A modular platform for cytocompatible hydrogels with tailored mechanical properties based on monolithic matrices and particulate building blocks. *Biomacromolecules*, *24*, 2755.
34. Brokesh, A. M., & Gaharwar, A. K. (2020). Inorganic biomaterials for regenerative medicine. *ACS Appl Mater Interfaces*, *12*, 5319.
35. Diba, M., Wang, H., Kodger, T. E., Parsa, S., & Leeuwenburgh, S. C. G. (2017). Highly elastic and self-healing composite colloidal gels. *Advanced Materials*, *29*.
36. Hassani Besheli, N., Martens, M., Macías-Sánchez, E., Olijve, J., Yang, F., Sommerdijk, N., & Leeuwenburgh, S. C. G. (2023). Unraveling the formation of gelatin nanospheres by means of desolvation. *Nano Letters*, *23*, 11091.

SUPPORTING INFORMATION

Additional supporting information can be found online in the Supporting Information section at the end of this article.

How to cite this article: Maciel, M. M., Hassani Besheli, N., Correia, T. R., Mano, J. F., & Leeuwenburgh, S. C. G. (2024). Encapsulation of pristine and silica-coated human adipose-derived mesenchymal stem cells in gelatin colloidal hydrogels for tissue engineering and bioprinting applications. *Biotechnology Journal*, *19*, e2300469. https://doi.org/10.1002/biot.202300469